Landscape Ecol (2016) 31:2097–2114
DOI 10.1007/s10980-016-0384-8

RESEARCH ARTICLE

Landscape-scale characteristics of forest tornado damage in mountainous terrain

Jeffery B. Cannon · Jeffrey Hepinstall-Cymerman · Christopher M. Godfrey · Chris J. Peterson

Received: 16 December 2015 / Accepted: 11 April 2016 / Published online: 9 July 2016

Abstract
Context Landscape patterns created by natural disturbance such as windstorms can affect forest regeneration, carbon cycling, and other ecological processes.
Objectives We develop a method for remotely measuring tornado damage severity and describe landscape-scale patterns of tornado damage. We examine the extent and distribution of damage severity and gaps created by tornadoes, and examine how topographic variation can influence tornado damage severity.
Methods Focusing on two April 2011 tornadoes that struck the Chattahoochee National Forest (CNF) in Georgia and the Great Smoky Mountains (GSM) in Tennessee, we used supervised classification of aerial photographs to map damage severity. We report the extent and distribution of damage severity from each track and characterize patterns of damage using FragStats. Using topographic overlays, we test hypotheses regarding how physiographic features such as valleys and ridges affect tornado damage severity.
Results Tornado damage severity estimates were significantly correlated with ground-truth measurements. The 64-km CNF track damaged 1712 ha (>25 % severity), while the 26-km GSM track damaged 1407 ha. Tornado damage severity was extremely variable and frequency of gap sizes drastically decreased with size, with many small gaps and few very large gaps, consistent with other types of wind damage. Damage severity declined as tornadoes ascended ridges and increased as they descended ridges. This effect was more consistent on shallow slopes relative to steeper slopes.
Conclusions This study outlines an objective methodology for remotely characterizing tornado damage severity. The results from this study fill an important gap in ecological understanding of the spatial components of the forest tornado disturbance regime.

Electronic supplementary material The online version of this article (doi:10.1007/s10980-016-0384-8) contains supplementary material, which is available to authorized users.

J. B. Cannon (✉) · C. J. Peterson
Department of Plant Biology, University of Georgia, 2502 Miller Plant Sciences, Athens, GA 30602, USA
e-mail: jbcannon.pubs@gmail.com

Present Address:
J. B. Cannon
Colorado Forest Restoration Institute, Colorado State University, 126 Forestry Building, 1472 Campus Delivery, Fort Collins, CO, USA

J. Hepinstall-Cymerman
Warnell School of Forestry and Natural Resources, University of Georgia, 180 E. Green St., Athens, GA 30602, USA

C. M. Godfrey
Department of Atmospheric Sciences, University of North Carolina at Asheville, 231 Robinson Hall, CPO #2450, Asheville, NC 28804, USA

Keywords Blowdown · Disturbance · Landscape pattern · Remote sensing · Topography · Tornado damage

Introduction

Natural disturbances such as hurricanes, floods, fires, insect outbreaks, and tornadoes affect nearly every forested ecosystem and can create large, disturbed forest gaps (Lorimer 1980; Canham and Loucks 1984). Disturbance from wind damage is widespread, affecting an estimated 1.65 million ha of forest annually in the U.S. (Dale et al. 2001). In April 2011, the largest tornado outbreak ever recorded in the U.S. spawned over 200 confirmed tornadoes over four days (NOAA 2011). Extreme forms of wind damage from tornadoes and hurricanes affect many ecological processes in forests such as regeneration patterns (Peterson and Pickett 1995) and carbon cycling (Chambers et al. 2007; Dahal et al. 2014). At smaller scales, the uprooting of trees characteristic of wind damage can create pit-and-mound microsites, which maintain tree and herb diversity (Beatty 1984; Ulanova 2000), alter patterns of herbivory (Krueger and Peterson 2006), and influence soil respiration (Millikin and Bowden 1996).

Natural disturbance regimes are typically defined by the type of disturbance, magnitude, spatial factors (e.g., area, shape, and spatial distribution), and temporal factors (e.g., duration and frequency, Pickett and White 1985; White and Jentsch 2001). Some aspects of disturbance regimes, such as the extent, distribution of damage severity, and spatial patterns of damage can be characterized at the level of individual disturbances. Spatial patterns of forest damage include attributes such as typical gap size, shape, and spatial arrangement of gaps—each of which can have particular ecological effects. Forest gap size can influence seedling establishment, growth, and influence species diversity of the regenerating stand (Gray and Spies 1996; Schnitzer and Carson 2001). The spatial pattern or arrangement of gaps (also called gap structure or configuration) can influence ecological processes such as seed dispersal and regeneration (Turner et al. 2003).

Typical forest gap sizes are well-characterized for some natural disturbances such as gaps created by individual tree death (Runkle 1982), hurricanes (Foster and Boose 1992), thunderstorms (Webb 1989; Waldron and Ruel 2014), and straight-line winds (Nowacki and Kramer 1998; Lindemann and Baker 2001). Despite the frequency and ubiquity of tornadoes in the eastern United States, little is known about the landscape patterns tornadoes create. Although two remote sensing studies report on the extent of damage from particular tornadoes (Yuan et al. 2002; Wilkinson and Crosby 2010), these studies do not report important landscape patterns created by tornadoes such as the distribution of gap sizes, severity of damage within gaps, or gap configuration (Foster et al. 1998). Characterizing these spatial components of tornado disturbances complements parallel work after hurricanes, thunderstorms, and straight-line winds, and fills a major gap in our knowledge of the wind disturbance regime. Documenting the extent, severity, and spatial arrangement of damage to forests from tornadoes will contribute to a better understanding of the range of variability of tornado impacts on forests as well their ecological significance (Vaillancourt et al. 2009).

In addition to informing ecological processes, studying patterns of forest tornado damage can increase meteorological understanding of tornadoes. Tornado damage patterns may be useful for indirectly studying and classifying tornado behavior (e.g., Beck and Dotzek 2010). Doppler radar is rarely used to study tornadoes in mountainous, forested regions, because of limited accessibility and visibility in rugged terrain. Thus knowledge about how variables such as tornado intensity respond to changes in elevation, slope, and aspect is limited (Bluestein 2000). Analyses that relate tornado damage severity to topographic variation may inform meteorological descriptions of tornado behavior in mountainous terrain.

Objectives and hypotheses

In this study, we examine two of the over 200 confirmed tornadoes that were spawned during the 25–28 April 2011 outbreak. One of these tornadoes damaged parts of the Chattahoochee National Forest (CNF) in northern Georgia, and another struck the Great Smoky Mountains National Park (GSM) in eastern Tennessee. These study sites were chosen due to interest by park management, availability of aerial imagery, and to complement other ecological and

meteorological studies in these sites (Godfrey and Peterson 2014; Nagendra and Peterson 2015). Using digital aerial photographs, we mapped damage severity from each storm track. With the resulting map of damage severity, we tested five hypotheses related to spatial patterns of tornado damage and its interaction with topography.

Despite the apparent linear pattern of tornadoes (Foster et al. 1998), we expected tornado damage to be highly variable with respect to damage severity distribution, gap size, and gap shape. Tornadoes are often described by a Rankine vortex, where wind speeds decrease exponentially with distance from the outer vortex wall (Holland et al. 2006). Thus, we expect that the area affected decreases rapidly with increasing tornado intensity—with most areas receiving very low damage severity, and only a very small fraction receiving the highest level of damage severity. As with other types of windstorms such as hurricanes and thunderstorm winds, we expect that tornadoes will create gap sizes that follow a distribution with numerous small gaps, and few very large gaps (e.g., Lindemann and Baker 2001; Rebertus and Meier 2001; Xi et al. 2008).

We also used the severity map to test hypotheses relating forest damage severity to specific physiographic features. As tornadoes travel along valley bottoms or through mountain gaps, the Venturi effect may force tangential velocities to increase as the width of the valley or gap narrows, constricting the flow, while wind speeds should diminish when the valley widens (Fig. 1a). At least one observational study (Forbes 1998) suggests that tornado intensity may increase on the downslope side of a ridge due to vortex stretching and the requisite conservation of angular momentum. Thus, we expect that as a tornado passes over a ridgeline, damage severity will be greater on the leeward/rear aspect of slopes relative to the windward/front aspect (Fig. 1b). According to simulation models of tornado behavior including topography (Lewellen 2012), tornadoes are expected to weaken when ascending slopes and strengthen when descending slopes due to the topographic influence on corner flow swirl ratios, as also observed by Forbes (1998). Thus, we expect tornado damage severity to decrease with locally increasing elevation along the tornado track (Fig. 1c). This expectation has been supported by radar evidence from three tornado tracks (Lyza and Knupp 2014).

Methods

Damage classification and verification of aerial photographs

Three months after tornado damage, digital aerial photographs (3-band, true color, 20 cm resolution) were taken of each tornado track and ortho-rectified using a 10-m digital elevation model (U.S. Geological Survey 2015). To determine the damage severity from photographs, we classified each photograph into damage categories using supervised classification. We trained the classification with 400-m^2 training plots distributed across the extent of each tornado track. The plots were stratified so that half were in completely unaffected areas (margins of the photograph), and half were concentrated near the damaged portions of the photographs (Fig. 2a). We distributed 1200 training plots over the CNF track (approximately

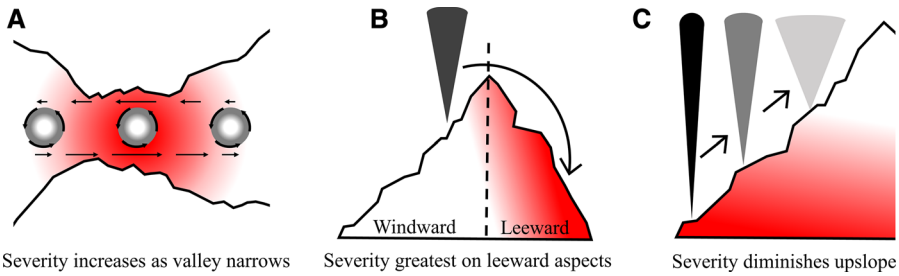

Fig. 1 Illustration of hypotheses of tornado behavior. **a** As a tornado vortex passes through a narrow valley or mountain gap, damage severity is expected to increase. *Arrows* represent wind field vectors. **b** As tornadoes pass over ridges, leeward slopes may be subject to more intense winds. **c** As tornadoes move uphill, tornado damage severity may decrease. Areas *shaded* in *red* are expected to receive higher wind velocity. (Color figure online)

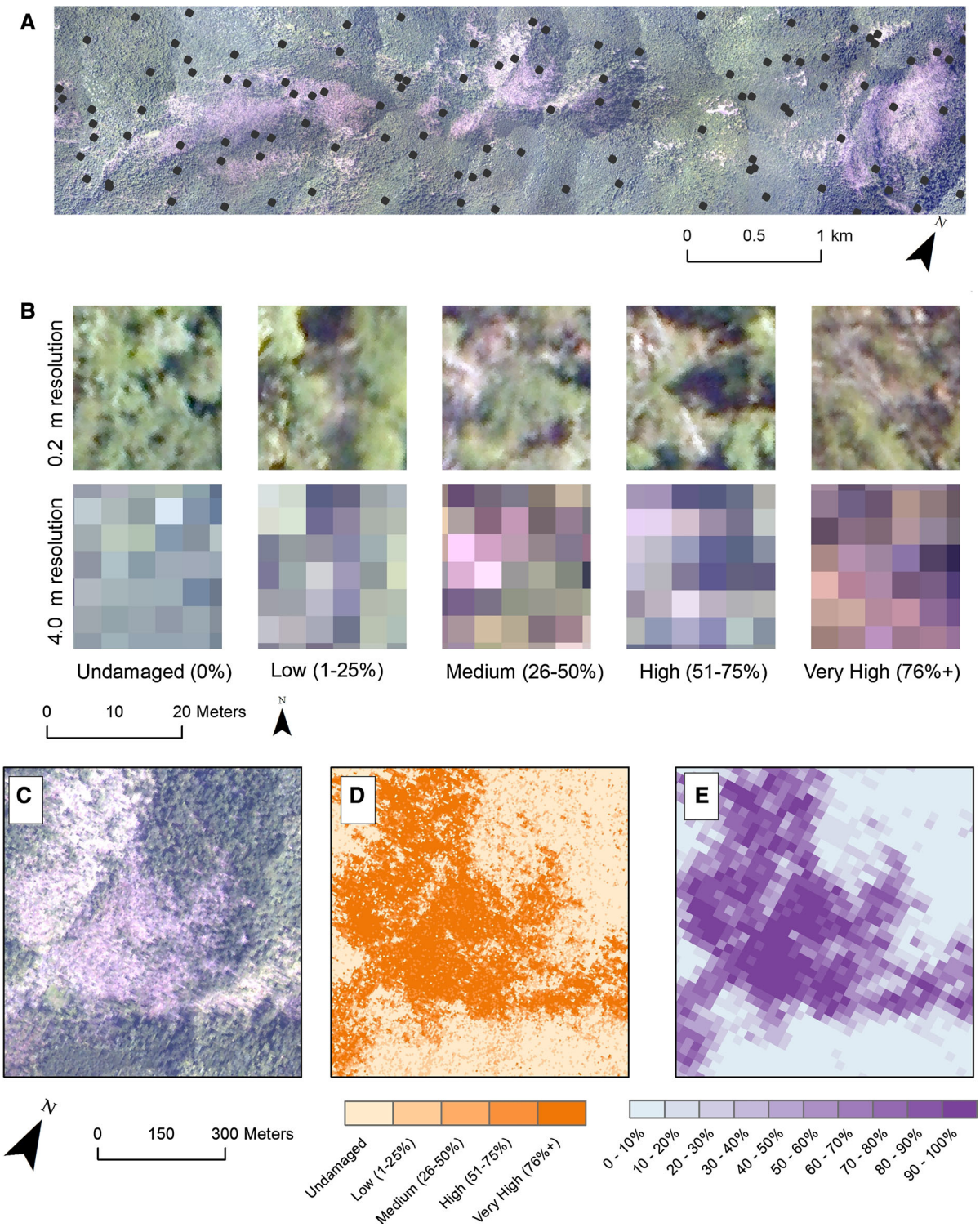
A
0
0.5
1 km
N
B
0.2 m resolution
4.0 m resolution
Undamaged (0%)
Low (1-25%)
Medium (26-50%)
High (51-75%)
Very High (76%+)
0
10
20 Meters
N
C
D
E
N
0
150
300 Meters
Undamaged
Low (1-25%)
Medium (26-50%)
High (51-75%)
Very High (76%+)
0 - 10%
10 - 20%
20 - 30%
30 - 40%
40 - 50%
50 - 60%
60 - 70%
70 - 80%
80 - 90%
90 - 100%

◀**Fig. 2** **a** Aerial photograph of a portion of tornado damage in the Chattahoochee National Forest (CNF) and stratified random placement of training plots (*black dots*) across the photograph used for the classification. **b** Examples of training plots overlaid on the imagery used in the classification. Each plot was visually assigned to one of five damage categories. The *top row* is a higher resolution (0.2 m) photograph used to visually classify training plots and the *second row* is lower resolution (4.0 m) used for the supervised classification. **c** Representative damage image. **d** Classification of the damaged area shown in **c**. **e** Estimate of tornado damage calculated by averaging 25 pixels in 400-m^2 blocks from the classification shown in **d** (Color figure online)

64 km long) and 700 plots over the GSM track (approximately 26 km long), corresponding to an areal coverage of 0.5 % of each track. Each training plot was visually interpreted from high resolution (20 cm) imagery into one of five disturbance classes based on the opinion of one of the authors (CJP) at a consistent map scale (1:8000). Training plots were interpreted prior to the remaining steps of the analyses based on the estimated percentage of basal area (BA) visibly felled using the following categories: undamaged (0 % BA down), low (1–25 % BA down), medium (26–50 % BA down), high (51–75 % BA down), and very high (76–100 % BA down). See examples shown in Fig. 2b, top row). While the visual interpretation was based on photo interpretation, it was based on >25 years of experience studying severe wind damage to forests, and, because it was prior to the other steps, all of the remaining steps were entirely objective.

The resolution of photographs was reduced from 20 cm to 4 m on each of three bands by average reflectance values to reduce the influence of shadows and produce a better spatial representation of wind damage (Fig. 2b, bottom row). We used supervised classification in ArcMap (ESRI 2011) to classify each pixel in the photographs. The classification process is illustrated in Fig. 2c–e. The classification uses the spectral signature of training plots within each class to classify the remaining pixels using maximum likelihood classification. The procedure classified each 16 m^2 pixel into one of the five damage classes (Fig. 2d). The midpoint damage severity was assigned to each pixel (undamaged = 0 %, low = 12.5 %, medium = 37.5 %, high = 62.5 %, and very high = 87.5 %) and blocks of twenty-five 16 m^2 pixels were averaged into 400-m^2 non-overlapping blocks. Because damage classification using severity class midpoints resulted in the highest classes reaching only 87.5 % severity, we rescaled estimates by dividing by 0.875 to produce a continuous estimate of damage severity from 0 to 100 % at a resolution of 20 m (Fig. 2e).

The basic classification above was combined with an approach that allowed for the use of *k*-fold internal cross-verification of the classification. For each track, we classified the photograph as above using a subset (80 %) of the training plots and withholding a smaller subset (20 %) to internally verify each classification. Because the training plots were categorical (e.g., low damage = 1–25 %), and the classification produced a continuous estimate of damage severity (e.g., 12 %), we used fuzzy class boundaries, considering training plots classified within ±10 % of the visual interpretation as accurately classified using the methodology outlined in Congalton and Green (2009). The classification was repeated five times for each track, withholding a different set of training plots for verification in each instance. This resulted in five estimates of damage severity for each track that were averaged together to produce a single damage severity map for each track (Figs. 3, S1).

In addition to the internal verification described above, we also conducted an out-of-sample validation of the remotely sensed map classification using ground-truth plots. At the CNF and GSM sites, we collected measurements of the percentage of basal area down (severity) in 400-m^2 ground plots—38 from CNF and 34 from GSM in the summers of 2012 and 2013. The size of ground plots was chosen to coincide with the desired resolution of the damage severity map (20 m). To validate the damage severity map, ground measurements of damage severity were related to those estimated by the classification of each tornado track in the corresponding area of the photograph using separate simple linear regressions for each site.

Tornado damage extent and distribution

The final damage map consisted of a continuous estimate of basal area down ranging from 0–100 % (See Figs. 3, S1). We estimated the area of land affected by each tornado by calculating the amount of land receiving >25 and >50 % damage severity. To place the affected area into context, we compared the area affected from the CNF and GSM tornadoes to

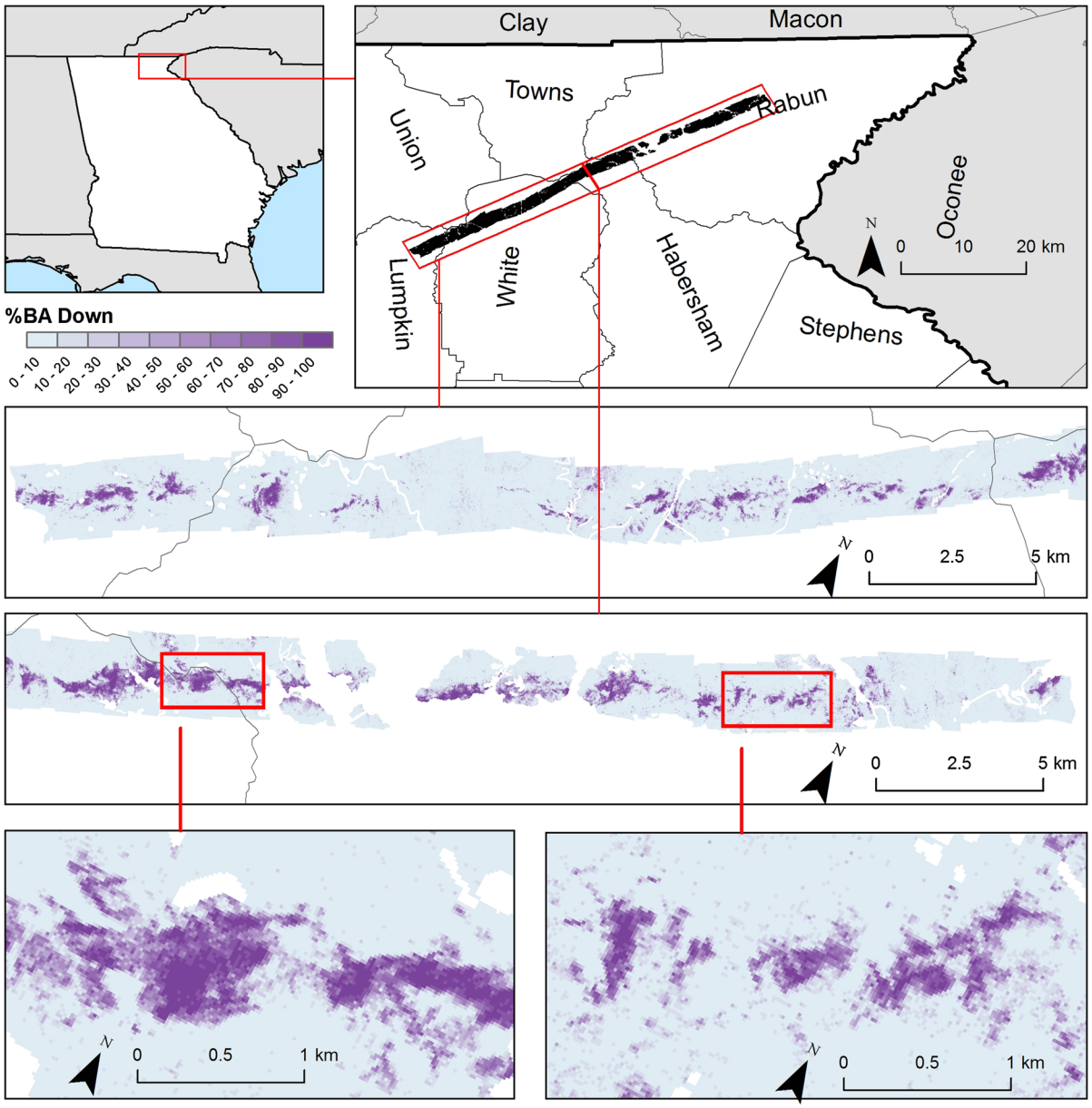

Fig. 3 Map of tornado damage severity from the April 2011 tornado that struck the Chattahoochee National Forest (CNF) in northeastern Georgia. Note that the lower four *insets* are rotated 28 degrees clockwise. Lowest two *insets* compare clusters of damaged patches in subsets of each tornado track. Areas missing from maps represent areas not included in the aerial imagery or areas of non-forest (lakes, streams, roads, wildlife cuttings, etc.) (Color figure online)

other recorded tornadoes. The severe weather reports database managed by the National Oceanic and Atmospheric Administration's Storm Prediction Center (SPC) Severe Weather Database Browser includes the estimated lengths and widths of all recorded tornadoes from 1950 to 2014 (http://www.spc.noaa.gov/climo/online/sp3/plot.php). Using the length and width dimensions from recorded storms, we estimated the typical area affected by tornadoes assuming tornado tracks were rectangular (when average tornado path width was reported, pre-1995) or rhomboidal (when maximum path width was reported, post-1995).

We then compared the area affected by the CNF and GSM tornado tracks to the distribution of the area affected by historical tornadoes rated on the Enhanced Fujita (EF) scales as EF3 or EF4.

To examine the distribution of tornado damage severity, we created histograms representing the area of damage in each damage severity class. We also characterized the distribution of gap sizes using FragStats 4.0 to describe the distribution of gap sizes created by tornado damage. We considered continuous areas with >10 % damage as gaps and areas ≤10 % damage severity as non-gaps (McGarigal et al. 2012).

Characterization of landscape patterns

We reclassified the damage severity map into four categories: low (10–25 %), medium (26–50 %), high (51–75 %), and very high (76–100 %) to facilitate characterization of spatial patterns using FragStats (McGarigal et al. 2012). We measured landscape metrics that would characterize important components of landscape heterogeneity (Li and Reynolds 1994). The metrics calculated within each damage class included (1) the number of patches, (2) mean size of patches, (3) mean patch shape index, an index that increases with patch shape complexity calculated as $S_i = 0.25 \cdot P_i \cdot a_i^{-0.5}$, where S_i is the shape index of patch i, P_i is the perimeter (m) of patch i, and a_i is the area (m^2) of patch i (McGarigal et al. 2012), and (4) mean edge-to-edge distance to the nearest patch of the same type (nearest neighbor distance), a measure of patch aggregation.

Topographic influence on tornado damage severity

We used overlay analyses to test how topographic features such as valleys and ridges influence tornado damage severity. Each analysis below utilizes a 30-m digital elevation model overlaid with tornado damage severity to relate changes in topography (elevation or slope) to changes in damage severity in particular physiographic settings such as valleys and ridges.

To examine whether tornado severity increased when passing through narrow portions of valleys (Fig. 1a), we identified portions of each tornado track where the tornado path traveled through a valley bottom and delineated each valley along the ridges parallel to the tornado path. We created a series of adjacent 150 × 150 m virtual sampling plots along the tornado path and measured the valley width at each plot (Fig. 4a). We included any valleys where the path length was at least 300 m, resulting in six valleys identified in the CNF track and four at the GSM site (See Table S1 for details). Within each plot, we calculated the mean tornado damage severity (Fig. 4b). To determine whether changes in valley width were correlated to changes in damage severity, we calculated the difference in valley width (Δ_{valley}) and the difference in severity ($\Delta_{severity}$) between adjacent sampling plots and related the measurements using simple linear regression, pooling data for all valleys.

To test whether the intensity of tornadoes increases on the leeward side of ridges (Fig. 1b), we examined areas where tornadoes ascended and descended a ridge perpendicular to the ridgeline. In these areas, we compared tornado damage severity on windward and leeward slopes. We identified portions of each tornado track where the tornado path traveled perpendicular to a ridge and delineated each ridge, placing adjacent 150 × 150 m sampling plots on the windward and leeward slopes of each ridge (Fig. 4c). We included all ridges where each aspect was at least 150 m long to allow the placement of at least one sampling plot on each ridge aspect. The sample included 10 ridges from the CNF track and 6 from the GSM track (See Table S2 for details). To aid in the identification of ridges running perpendicular to the tornado track, we calculated an exposure index for each pixel on the digital elevation model [cos(slope direction − tornado path direction − 180°)]. This index contrasted the windward (upslope) and leeward (downslope) aspects of ridges—with windward aspects having large values (+1), and leeward aspects having low values (−1)—allowing ridges perpendicular to the tornado path to be identifiable (Fig. S2). We calculated the mean tornado damage severity in regions contained within subplots for windward and leeward aspects of each ridge (Fig. 4d), pooling severity data for subplots on a given aspect. We used a one-tailed paired t test to test the hypothesis that tornado damage severity was greater on leeward facing ridge aspects than windward facing ridge aspects, which is the expectation if vortex stretching plays a large role.

To test whether tornado damage diminishes as tornadoes ascend slopes and increases while moving downslope, we correlated elevation changes along ridges to changes in damage severity. Using data from the same set of ridges as in the previous hypothesis (Table S2), we calculated the change in elevation

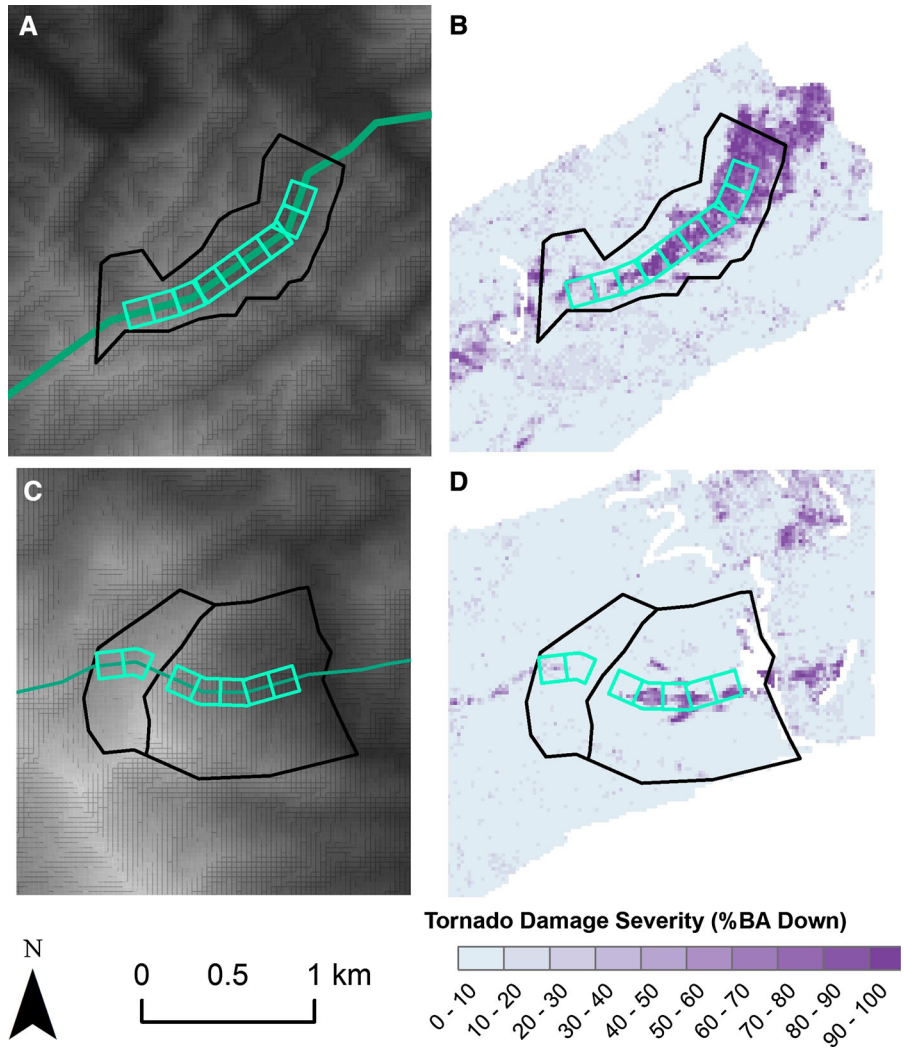

Fig. 4 **a** Portion of Great Smoky Mountains (GSM) tornado track where tornado path (*blue line*) passed through valley bottom showing the outline of adjacent ridges and transects for measuring valley width. **b** Same portion of GSM track as in A with map of severity overlaid showing sampling areas (*light rectangles*). **c** Portion of Chattahoochee National Forest (CNF) tornado track where tornado path passed over a ridgetop showing uphill (*left*) and downhill (*right*) portions. **d** Same portion of CNF track as in **c** with map of severity overlaid showing sampling areas (*light rectangles*). *White areas* in **b** and **d** represent roads, streams, or other non-forest where damage severity was not estimated. (Color figure online)

($\Delta_{elevation}$) and the change in severity ($\Delta_{severity}$) between adjacent subplots on each ridge, and related the measurements using simple linear regression. Because $\Delta_{elevation}$ and $\Delta_{severity}$ require at least two subplots to calculate a difference, we only included ridges that contained at least two subplots on both upslope and downslope aspects, resulting in the inclusion of nine ridges in the analysis (all from the CNF track in Table S2). After finding a significant effect of elevation change on damage severity, we further explored whether the size of this effect differed on shallow and steep ridges. We calculated the correlation coefficient of $\Delta_{elevation}$ and $\Delta_{severity}$ for each ridge and regressed this coefficient against the mean slope of individual ridges.

Results

Verification of aerial photograph classification

The aerial photograph classification produced estimates of damage severity illustrated in Figs. 3 and S1. Internal verification comparing visual interpretation of the training plots to the resulting severity map indicated that the classification performed well with 1127 of 1206 (93.4 %) of CNF training plots accurately classified within ±10 % of the visual interpretation of those plots; similarly, 590 of 667 GSM training plots (88.5 %) were accurately classified (Tables S3, S4, respectively). Producer accuracies for CNF ranged from 78 to 95 % and from 77 to 88 %

for GSM. User accuracies ranged from 80 to 100 % for CNF and from 76 to 100 % for GSM. In general, accuracies were highest for the higher and lower severity classes and lowest for the intermediate severity classes. Ground-truth measurements of damage severity were significantly correlated to the corresponding estimates from the severity map for both CNF ($p < 0.001$, $r = 0.775$) and GSM ($p < 0.001$, $r = 0.640$).

Tornado damage extent

The CNF tornado track produced considerable damage with 1003 ha receiving damage >50 % severity over the 64 km length of the track. An area of 1712 ha was damaged >25 % and an area of 2914 ha was damaged >10 %. The GSM tornado damaged 743 ha > 50 %, 1407 ha > 25 %, and 2678 ha > 10 %. Figure 5 illustrates the amount of land area affected by each tornado in damage class bins of 10 % (see also Table S5).

The analysis of historical tornadoes showed that damage extent for EF3 and EF4 tornadoes was highly skewed, with estimates of damage for EF3 tornadoes over 29,000 ha with a mean of 799 ha and a median of 235 ha. Damage extent from EF4 rated tornadoes reached 33,800 ha with a mean of 2201 ha and a median of 830 ha in damaged area (See Table S6 for details). The 1712 ha damaged (>25 %) by the CNF tornado places it at the 89th percentile of area affected among EF3 tornadoes. Similarly, these estimates place the GSM tornado (1407 ha, >25 % damage) at the 63rd percentile among historical EF4 tornadoes.

As expected, tornado damage was extremely heterogeneous across the landscape. Visual inspection of the histograms of area affected by damage severity (Fig. 5) supported the expectation of a rapid decrease in area affected by increasing damage severity. However, a variety of goodness-of-fit tests indicate that the data do not follow any common parametric distributions (e.g., gamma, negative exponential). The amount of land area damaged decreased rapidly in the range of 0–40 % (minor damage). However, in the higher levels of damage severity (40–100 %), approximately equal amounts of land area were distributed among each damage severity class (Fig. 5).

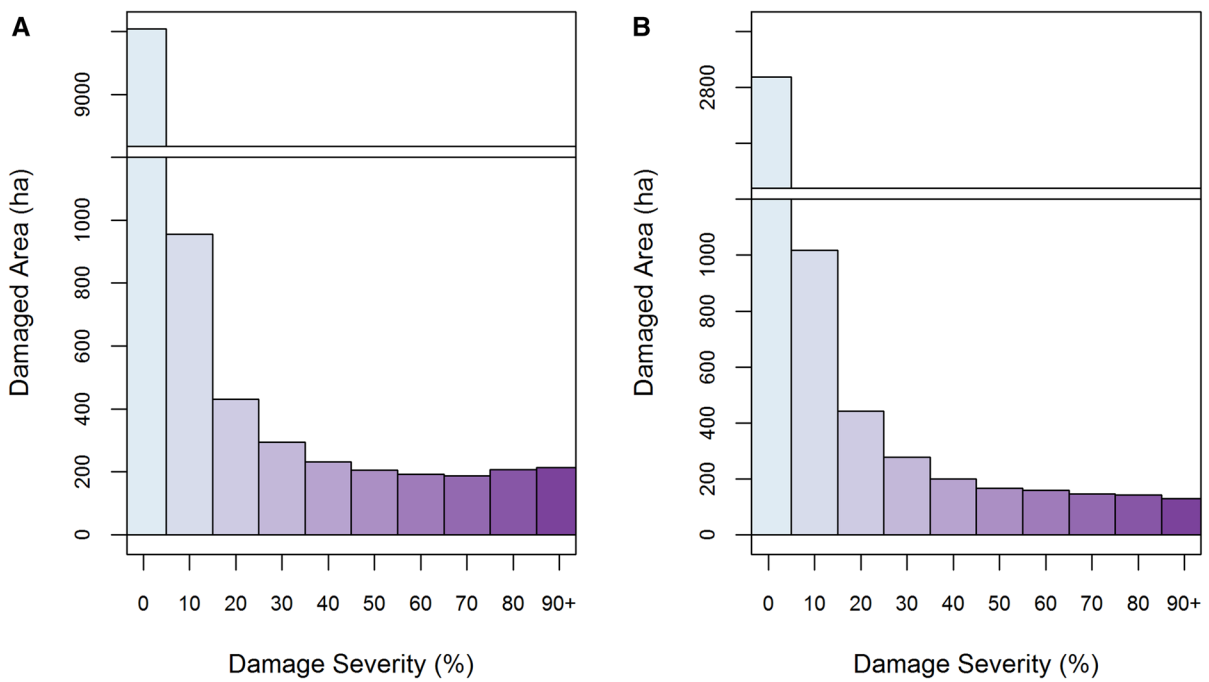

Fig. 5 Distribution of damage severity extent for **a** Chattahoochee National Forest and **b** Great Smoky Mountains tornado tracks. Note break in *y*-axes at 1200 ha (Color figure online)

Landscape patterns of tornado damage and gap size distribution

The frequency of gap sizes for CNF and GSM also decreased dramatically with increasing gap size (Fig. 6). Mean gap sizes (±1 s.e.) for CNF and GSM were 0.568 ± 0.092 and 1.015 ± 0.316 ha, respectively. Owing to the very large number of very small gaps, minimum and median gap sizes for CNF and GSM were each 0.04 ha. The three largest gaps for CNF were 154, 159, and 207 ha; the three largest gaps for GSM were 338, 347, and 498 ha. As with the distribution of damage severity, although the distribution of patch size resembled a negative exponential, a variety of goodness-of-fit tests indicate that the data do not follow any common parametric distributions.

Considering landscape metrics of patch number, size, shape, and arrangement together suggests that tornado damage is distributed in a dissolved bull's-eye pattern (Figs. S3, 7). Overall, the number of patches decreased as damage severity increased (Fig. 7a, e; Tables S7, S8). Conversely, the size of patches increased with damage severity (Fig. 7b, f; Tables S7, S8). For CNF, patch shape was simpler in the highest and lowest damage severity classes, but more complex in patches with intermediate damage severity (Fig. 7c; Table S7). However, no clear pattern between patch severity and shape was detected for GSM (Fig. 7g; Table S8). Finally, the analysis showed that distance between like-patches increased significantly with damage severity class from about 53 m between patches in the lower damage severity class to 72 m between patches in the highest damage severity class at CNF (Fig. 7d; Table S7) and from 46 to 71 m at GSM (Fig. 7h; Table S8).

Effects of topography on damage severity

Tornado damage severity did not increase when valleys narrowed. There was no correlation between changes in valley width and changes in tornado damage severity (Fig. 8a, $R^2 = 0.004$, df = 70, p = 0.607). In fact, for individual valleys, the relationship between changes in valley width and damage severity was highly variable, ranging from a positive correlation (e.g., CNF-1 in Fig. S4) to a negative correlation (e.g., CNF-6 in Fig. S4). There was also no evidence that leeward aspects of ridges traversed by tornadoes had greater damage. Tornado damage was higher on windward ridge aspects (40.3 %) than leeward ridge aspects (32.6 %, Fig. 8b), but the difference was highly variable and not statistically significant (paired one-tailed $t = 1.257$, df = 15 p = 0.886).

Tornado damage severity decreased with increases in elevation (Fig. 9a, $R^2 = 0.143$, p = 0.001). In Fig. 9, note that positive values of $\Delta_{elevation}$ represent

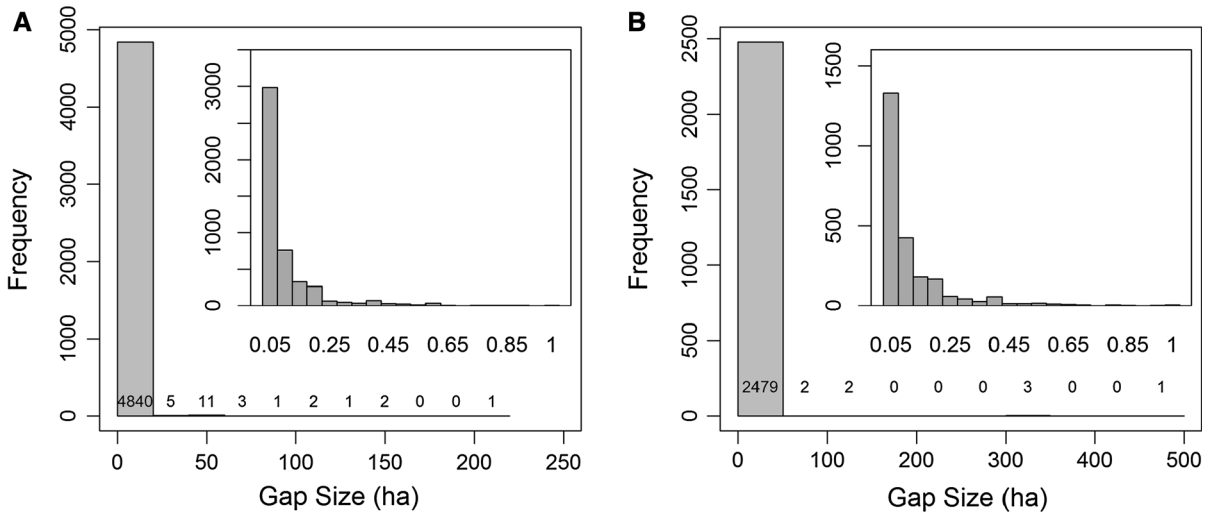

Fig. 6 Histogram of gap size distribution of **a** Chattahoochee National Forest and **b** Great Smoky Mountains tornado. Because most gaps (99.5 %) were ≤1 ha, *insets* in **a** and **b** show histogram for gaps ≤1 ha. Note the changes in the *y*- and *x*-axes between *panels a* and *b*

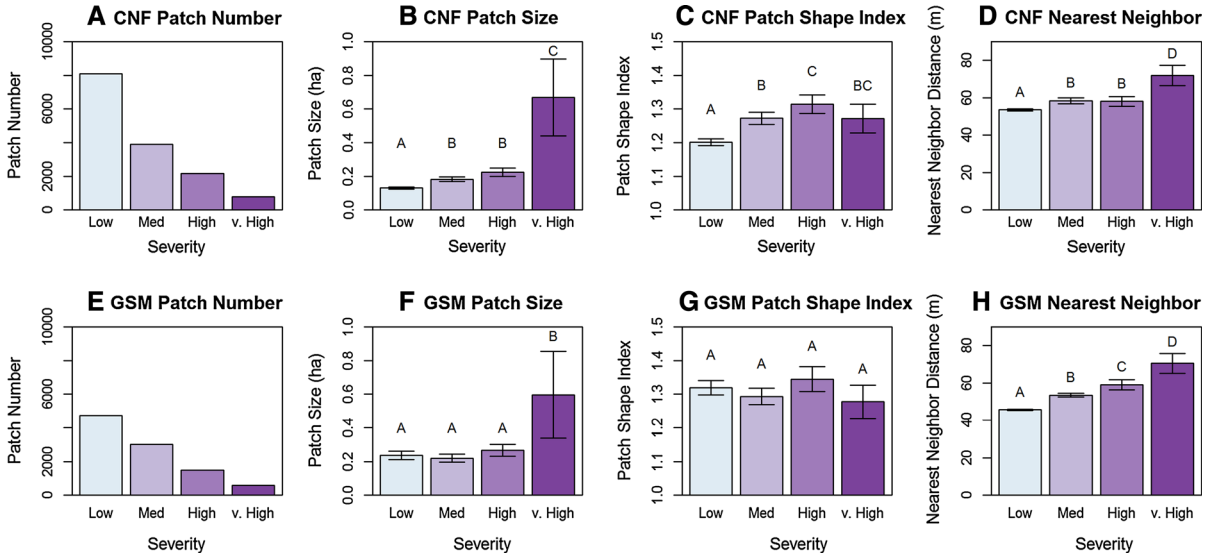

Fig. 7 Patch-based metrics by each damage severity class (low, medium, high, and very high) for CNF (**a**–**d**) and GSM (**e**–**f**). Number of patches (**a**, **e**). Mean patch size (**b**, **f**). Mean patch shape index (**c**, **g**). Mean nearest neighbor distance (**d**, **h**). *Error bars* represent ± 2 standard errors of the mean metric (Color figure online)

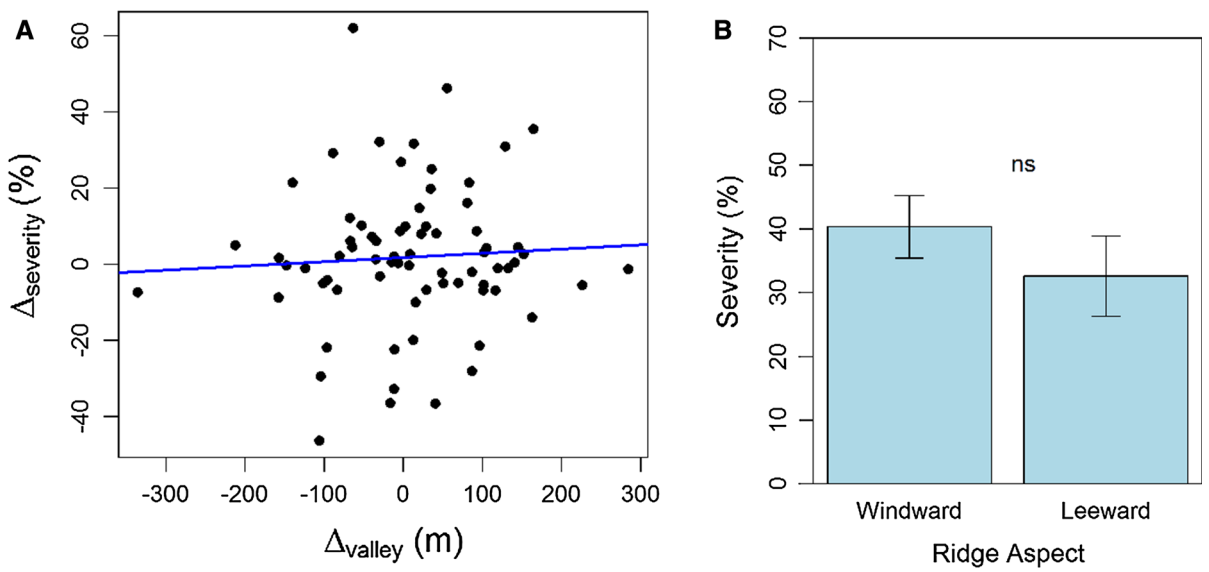

Fig. 8 **a** Scatterplot illustrating relationship between changes in valley width and changes in tornado damage severity. ($R^2 = 0.004$; $p = 0.607$). **b** Mean damage severity on windward and leeward aspects of ridges traversed by the Chattahoochee National Forest and Great Smoky Mountains tornadoes (paired t test, $p = 0.4173$)

subplots where the tornado traversed upslope and negative values represent subplots where tornadoes traversed downslope. Decreases in damage severity were typical when the tornado moved upslope while increases in tornado damage severity were typical when the tornado moved downslope. The overall regression coefficient of −0.21 indicates that increases of elevation of 100 m result in decreases in damage severity by approximately 21 percentage points. The relationship between $\Delta_{elevation}$ and $\Delta_{severity}$ was consistently negative for each of the nine individual ridges examined, with regression coefficients ranging from

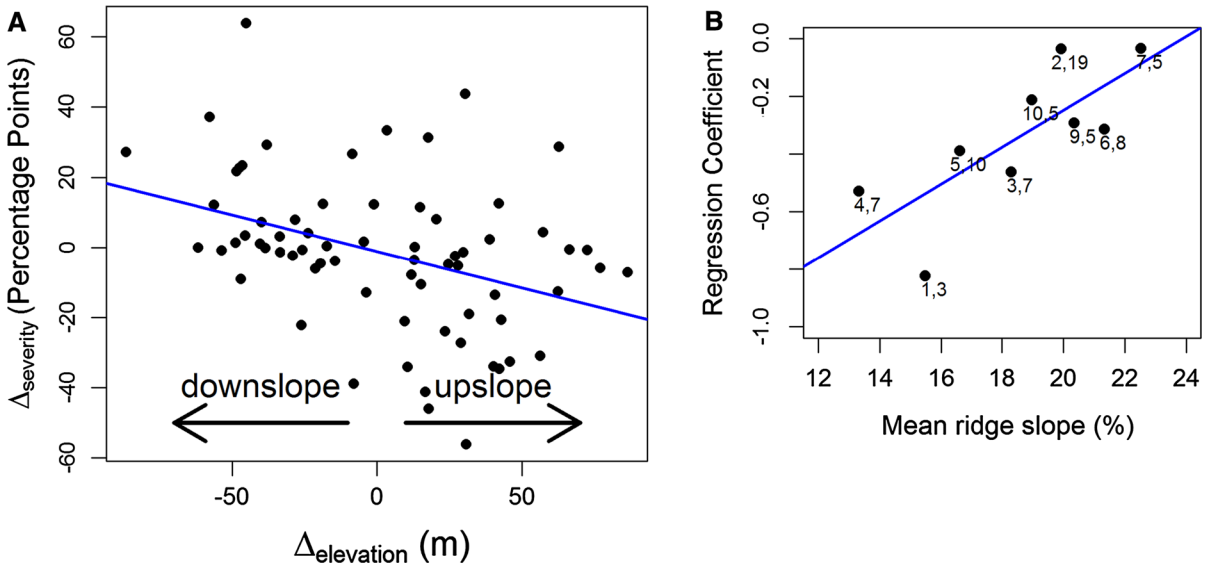

Fig. 9 **a** Scatterplot illustrating relationship between changes in elevation and changes in tornado damage severity ($R^2 = 0.143$, $p = 0.001$). Negative values of $\Delta_{elevation}$ represent portions of the tornado track where the tornado traversed downslope while positive values represents portions of the track where the tornado traversed upslope. **b** Linear regression illustrating the relationship between the mean slope of a ridge and the regression coefficient of $\Delta_{elevation}$ versus $\Delta_{severity}$ ($R^2 = 0.51$, $p = 0.018$). Lower regression coefficients (more negative) indicate stronger effect of elevation. *Point labels* indicate the identity of the ridge and the number of plots used for each coefficient, respectively (all ridges from CNF). See Fig. S5 for raw values

strongly negative (−0.82) to weakly negative (−0.03) with a mean coefficient of −0.34 (Fig. S5). The effect of $\Delta_{elevation}$ on $\Delta_{severity}$ was greater on ridges with shallower slopes relative to steeper slopes (Fig. 9b, $R^2 = 0.51$, $p = 0.018$).

Discussion

Tornado extent and distribution

The amount of forested area damaged by a single tornado is minute compared to the area affected by larger, infrequent natural disturbances such as the Mt. St. Helens eruption, the 1938 New England Hurricane, or the Yellowstone wildfires (Turner et al. 1994; Foster et al. 1998). However, the cumulative effect of hundreds of tornadoes during a tornado outbreak can affect a much larger spatial extent. The tornado outbreak of April 2011 produced over 200 detected tornadoes. In fact, large tornado outbreaks are quite common. In the U.S., approximately 18 days per year have tornado outbreaks where >1.5 % of the expected annual number of tornadoes occur or at least eight F1+ tornadoes occur (Verbout et al. 2006). Moreover, an estimated 1300 tornadoes occur in the U.S. each year (Storm Prediction Center 2012). Consequently, the cumulative spatial coverage of thousands of tornadoes may correspond with a substantial fraction of the area impacted by infrequent—though more dramatic—disturbances. Preliminary research suggests that tornadoes may damage as much as 300,000 ha of forest annually—an area nearly that of Rhode Island (CJ Peterson, JB Cannon, and LJ Snyder, unpublished data).

The potential area affected by a single tornado is highly variable, but it is corresponds with the intensity of the tornado (Brooks 2004). We estimate that the area affected by the CNF (EF3) and GSM (EF4) tornadoes rank in the 89th percentile and 63rd percentile, respectively, among tornadoes of the same damage rating (Table S6). One other study completed by Wilkinson and Crosby (2010) estimated the forest area affected by an April 2010 EF4 tornado that struck Mississippi. These authors found that nearly 17,000 ha received at least 'light' damage, corresponding to the 99th percentile among EF4 tornadoes.

Although these authors used remotely sensed satellite imagery to estimate the extent of damage, the criteria for thresholding damage severity as 'light', 'moderate, or 'severe' was not described.

Although there are recognized limitations to EF-scale ratings, and reports of path lengths (Doswell and Burgess 1988) the length and width data from the SPC remain the best resource for understanding the extent of previous tornadoes dating back to 1950. While track lengths and widths as reported by the National Weather Service can be used to calculate a very rough estimate of the areal extent of forest damage, it is problematic to use such an estimate when considering ecological processes for several reasons. First, such an areal calculation gives no indication of the level of damage severity the forest sustained (i.e., the proportion of trees downed). Second, the estimated area does not consider heterogeneous damage severity within tornado tracks, which was considerable in this study (Fig. 5). Lastly, damage survey teams may have trouble accessing remote regions following tornadoes that have passed through forests and therefore may rely on only a handful of widely-spaced ground observations to characterize such tornado tracks.

The technique to map tornado damage to forests remotely from aerial photographs as described here provides a straightforward and relatively objective method to map tornado extent as well as damage severity within a given track at a fine scale. Thus, we recommend adoption of this method in closed canopied forests, such as those in the eastern U.S., for making detailed measurements of tornado extent while explicitly incorporating the extreme spatial heterogeneity often present in tornado damage.

Gap size distribution

Gap sizes in our study exhibited a distribution with numerous very small gaps and few very large gaps. Several studies of windstorms report gap size distributions skewed toward small gaps, including hurricanes (Foster and Boose 1992; McNab et al. 2004; Xi et al. 2008), thunderstorm winds (Evans et al. 2007), blowdowns (Rebertus and Meier 2001), and downslope wind events (Lindemann and Baker 2001). Thus, a rapidly decreasing frequency of gaps with increasing size may prove to be a general property of windstorms. A mechanism explaining this pattern may be related to the fact that in many windstorms, including tornadoes, wind severity is low over much of the affected areas and only a small fraction of the area is affected by winds of high intensity. In areas experiencing low-intensity winds, small gaps may be created when only the most vulnerable trees, such as the largest trees (Peterson 2000), those with fungal rot (Matlack et al. 1993), or those previously fire-scarred (Cannon et al. 2015), are damaged. Such a mechanism would create small, low-severity gaps over a large area. However, in a few areas, extreme winds may overcome differences in vulnerability (Canham and Loucks 1984; Peterson 2000; Canham et al. 2001) resulting in more complete windthrow of trees and thus larger gap sizes in a smaller portion of the affected area. A positive correlation between damage severity and gap size (Peterson et al. 2013), combined with a negative correlation between gap size and gap number, may result in a relatively even distribution of damage severity across a blowdown.

In this study, gap sizes at CNF and GSM averaged 0.6 and 1.0 ha, respectively, which were most similar to those reported from Hurricane Opal damage to the Bent Creek Watershed (gap sizes of 0.6 ha in basin and 0.9 ha in highlands, McNab et al. 2004). Gap sizes from the CNF and GSM tornado tracks were also similar to those reported from blowdowns in the Missouri Ozarks (mean gap size 0.8 ha, estimated from Fig. 1 in Rebertus and Meier 2001) and those reported following Hurricane Fran (Xi et al. 2008; 0.01–1.1 ha Busing et al. 2009), although it should be noted these analyses were conducted at the stand-scale and used a stricter concept of gap size (Runkle 1982) rather than a threshold damage severity level, resulting in smaller gaps. Gap sizes in this study were much smaller than those gaps formed from the 1938 New England hurricane (estimated mean gap size is 3.5 ha, Fig. 6 in Foster and Boose 1992), and a Pennsylvania windstorm (mean gap size 4.78 ha, Evans et al. 2007). They were also much smaller than from a downslope wind event in the Rocky Mountains (mean 25.2 ha, Lindemann and Baker 2001).

The small and irregularly shaped gaps in this study starkly contrast with the gaps from the downslope wind event study (Lindemann and Baker 2001), which were larger and had simpler shapes. These differences in damage patterns could arise from differences between the wind disturbances themselves (tornado versus downslope wind event) or from differences in vegetation between the regions. For example, gaps in

the temperate Southern Appalachians may be more diffuse and irregular owing to the differences in windfirmness among the diverse trees, while gaps in the less-diverse subalpine forests of the Rocky Mountains may be larger and uniform. Although neither mechanism is explicitly supported by the Lindemann and Baker (2001) study, it is difficult to reject either hypothesis based on the patterns observed within a limited number of disturbances.

Landscape patterns of tornado damage

The analysis of landscape patterns produced by tornadoes resulted in a description of a putative pattern that may be characteristic of tornado damage. The results of the patch analysis are consistent with a dissolved bull's-eye pattern (Fig. S3; Tables S7, S8). In this pattern, a central area with severe damage is nested within less severely damaged patches that become broken-up, or dissolve, away from the center of the damaged area. The dissolved bull's-eye pattern is consistent with the positive correlation of patch size and severity, as well as the negative correlation of patch number and severity (Fig. 7). A similar size–severity correlation among forest gaps was also found in non-tornadic wind by Peterson et al. (2013). Lastly, adjacent damaged areas shaped like a bull's-eye create the dispersion pattern seen in Fig. 7d, h, with low damage severity areas with short nearest-neighbor distances and high severity areas dispersed with much longer neighbor distances.

Damage severity from these tornadoes was extremely heterogeneous, and although there was a large amount of land area exhibiting minor damage (10–20 %), approximately equal amounts of land area were affected by medium to higher (>30 %) levels of damage severity (Fig. 5). Heterogeneous damage with approximately equal amounts of land in each of the higher damage severity classes may be a general characteristic of some natural disturbances such as tornadoes. The fact that low-severity patches are small and numerous while high-severity patches are large and few (Fig. 7a, b) may result in approximately equal portions of the landscape in each damage severity class (Fig. 5).

A pattern with relatively even distributions of forested area among damage severity categories was found with the Yellowstone fires (Turner et al. 1993). Canham et al. (2001) observed that only a relatively small portion of land area received "catastrophic" damage from separate derecho blowdown events that struck the Adirondack Mountains and northern Wisconsin (Canham and Loucks 1984), but the study does not report area affected by intermediate levels of damage severity. A heterogeneous pattern of damage from tornadoes contrasts with that from other types of disturbances that exhibit damage patterns with damaged areas concentrated in the most severe classes such as the 1938 New England hurricane (Foster and Boose 1992) and a barrier-induced downslope wind event in the Rocky Mountains (Lindemann and Baker 2001). A greater meteorological understanding of different types of windthrow and how they interact with topography may shed light on the variations among damage patterns created by wind disturbances.

Topographic influences on tornado damage severity

Lastly, this study demonstrates that certain physiographic settings influence tornado damage severity. In several instances along the CNF and GSM tornado paths, tornadoes appeared to be channeled along valley bottoms, suggesting that topography can even influence the ground-level movement of the tornado to some extent, despite the relatively constant motion vector of the parent supercell thunderstorm. Based on the ten valleys we examined, however, we found no evidence to support the hypothesis that steadily narrowing valley widths lead to increased damage severity via the Venturi effect (Fig. 8a). Furthermore, our analysis of sixteen ridges did not support the hypothesis that aspects on the leeward side of ridges receive higher wind damage when a tornado passes over a ridge (Fig. 8b). Although an observational study by Forbes (1998) predicted greater damage from tornadoes on leeward aspects of ridges, it should be noted that a simulation study by Dotzek et al. (2011) has made the opposite prediction for supercell thunderstorms. The large variability of damage on windward and leeward aspects in our study precludes support of either of these hypotheses.

This analysis does support the hypothesis that tornado severity diminishes as tornadoes travel upslope and strengthens when they travel downslope (Fig. 9a), and this effect is stronger on shallow slopes (Fig. 9b). Vortex stretching can certainly help to explain some of this effect, but the fact that this effect is more apparent on shallow slopes may be more complicated. While a

complete analysis of such behavior is beyond the scope of this work, Lewellen's (2012) numerical simulations suggest that as a tornado climbs a hill, the combined effects of vortex compression and the deflection of the near-surface swirl flow component by the hill back toward the tornado can weaken the circulation. Yet these simulations indicate that many other factors can also influence this flow field as well, including translational velocity, surface roughness, and topography. Perhaps steeper slopes do not allow for a combination of such factors to act to modify the intensity of the tornado as it ascends or descends, while shallower slopes allow for such adjustments in intensification. Recently, radar evidence from three tornado tracks (Lyza and Knupp 2014) has provided further evidence of such upslope–downslope effects.

Previous landscape-scale studies of other types of windstorms have revealed general patterns of the effects of topography. The fact that topography influences wind damage severity is well-established for hurricanes. Higher slope wind exposure resulted in higher damage from the 1938 New England Hurricane, Hurricane Hugo (Foster and Boose 1992; Boose et al. 1994), Hurricane Opal (McNab et al. 2004), Hurricane Fran (Xi et al. 2008), and Hurricanes Charley, Katrina, Rita, Gustav, and Yasi (Negrón-Juárez et al. 2014). In some of these studies, other topographic factors have been correlated with higher hurricane damage severity, though not consistently. For example, Xi et al. (2008) found the greatest damage on ridge tops and valley bottoms, while McNab et al. (2004) found the greatest damage at low elevation with less damage on ridges. The effects of topography on other types of windstorms is even less consistent. Lindemann and Baker (2002) found that exposed, east-facing slopes were most vulnerable from a downslope wind event in the Rocky Mountains when winds traveling eastward damaged leeward slopes. Rebertus and Meier (2001) also found that leeward slopes were more heavily damaged from a blowdown in the Missouri Ozarks. While Lindemann and Baker (2002) found that flatter and shallow slopes displayed the highest level of damage, Evans et al. (2007) found that areas with higher slope variability experienced the greatest damage after a windstorm in Pennsylvania.

In these analyses of the effect of topography on tornado damage severity, we tested hypotheses of various tornado behaviors in specific topographic settings (e.g., ridges or valleys). This approach allowed the examination of specific tornado behaviors, and differs somewhat from previous analyses (e.g., Foster and Boose 1992) in which specific topographic variables (slope, elevation, and aspect) or combinations of topographic variables ("exposure") are correlated with damage severity at a large scale. For hurricanes, the scale of the storm dwarfs individual topographic features such as ridges. For tornadoes, the size of a tornado is more similar to the scale of individual ridges, thus a smaller-scale approach is necessary for analyzing topographic effects of tornadoes. To illustrate, if easterly winds from a hurricane damage two similar, adjacent hills, the exposed (eastern) aspect of each hill will likely be damaged while the leeward (western) aspect will likely be sheltered, and they will likely be damaged in a similar manner. However, in the same setting, a tornado may cross on the western side of one hill and the eastern side of the other. Thus, the windward and leeward sides of a tornado track are difficult to define at a landscape-scale, and instead should be defined and examined individually because the size of the tornado phenomenon is similar in scale to the size of the topography affecting it. This approach confirmed one purported behavior of tornadoes and may be useful for examining and testing additional hypotheses regarding how tornadoes move through complex terrain.

Analyses of tornado damage to forests inform tornado behavior in complex terrain, where accessibility, visibility, and availability of radar data are often limited. There is growing awareness among the meteorological community of the utility of remotely-sensed tree damage as important data sources for tornado intensity estimates (Godfrey and Peterson 2014; Peterson and Godfrey 2014). Unlike hurricanes, there is a paucity of studies on topographic influences on non-hurricane, non-tornado blowdowns, and even fewer studies on how tornado damage interacts with topography. Replicate studies using a similar methodology are needed in order to make stronger generalizations on the potential interactions between windstorms and topography. This study comparing two tornadoes is a step toward this goal, and it presents an objective methodology to apply toward future tornado studies.

Conclusion

Supervised classification offers a methodology to measure tornado damage severity remotely and at a

landscape scale. Such estimates allow characterization of landscape-scale patterns of tornado damage. Using this method, we found that the two examined tornadoes are extremely heterogeneous with roughly equal proportions of land area in high-, medium- and low-severity patches. Consistent with other types of wind damage, gap sizes resulting from tornado damage exhibit a size distribution with many small gaps and a few very large gaps. Lastly, tornado damage has complex interactions with topography, which can be explored using remote sensing methods.

Comparing specific values of landscape metrics across studies can be problematic because aspects of image processing may vary with differences in image interpretation, minimum recognized patch size, resolution of severity classes, and the spatial resolution of data (Turner et al. 2003). Therefore, one should be cautious drawing strong conclusions between studies with differing methodologies. The method we outline herein allows for remote measurement of tornado damage severity, extent, and pattern at a relatively high resolution (20 m). As with other studies that classify remotely-sensed imagery, this method still requires expert interpretation of training plots used in classifying the imagery. Nevertheless, the methodology improves upon previous efforts for remote measurement of tornado damage. First, the method uses high resolution aerial imagery which allows for higher resolution mapping of tornado damage severity compared to studies that used NDVI-based assessments from LANDSAT, which are limited to 30 m resolution. Second, this method results in finer damage resolution (e.g., 0–100 % severity) compared to other methods which result in much coarser estimates of damage (e.g., low, medium, high; Wilkinson and Crosby 2010). Thus, we recommend that future landscape-scale studies of wind damage to forests utilize a common methodology such as the one herein, which is both objective and large in spatial extent, to allow comparison and generalization between studies

Acknowledgments The authors would like to thank Paul Super, Tom Troutman, and the staff of Great Smoky Mountains National Park for their support and cooperation and all who participated in fieldwork including Michael Bailey, Meredith Barrett, Patrick Johnson, Sophia Kim, Uma Nagendra, Nick Richwagen, Luke Snyder, and Andrei Stanescu. We also thank Daniel Markewitz, Richard Lankau, Joseph O'Brien, and three anonymous reviewers for their helpful comments on the manuscript. This study was made possible by grants from the National Park Service's Climate Change Youth Initiative and the University of Georgia, Department of Plant Biology, and by grants from the National Science Foundation in Ecology (DEB1143511) and Meteorology (AGS1141926).

References

Beatty SW (1984) Influence of microtopography and canopy species on spatial patterns of forest understory plants. Ecology 65:1406

Beck V, Dotzek N (2010) Reconstruction of near-surface tornado wind fields from forest damage. J Appl Meteorol Climatol 49:1517–1537

Bluestein HB (2000) A tornadic supercell over elevated, complex terrain: the divide, Colorado, storm of 12 July 1996. Mon Weather Rev 128:795–809

Boose E, Foster D, Fluet M (1994) Hurricane impacts to tropical and temperate forest landscapes. Ecol Monogr 64:369–400

Brooks H (2004) On the relationship of tornado path length and width to intensity. Weather Forecast 19:310–319

Busing RT, White RD, Harmon ME, White PS (2009) Hurricane disturbance in a temperate deciduous forest: patch dynamics, tree mortality, and coarse woody detritus. Plant Ecol 201:351–363

Canham CD, Loucks OL (1984) Catastrophic windthrow in the presettlement forests of Wisconsin. Ecology 65:803–809

Canham CD, Papaik MJ, Latty EF (2001) Interspecific variation in susceptibility to windthrow as a function of tree size and storm severity for northern temperate tree species. Can J For Res 31:1–10

Cannon JB, Barrett ME, Peterson CJ (2015) The effect of species, size, failure mode, and fire-scarring on tree stability. For Ecol Manag 356:196–203

Chambers JQ, Fisher JI, Zeng H, Chapman EL, Baker DB, Hurtt GC (2007) Hurricane Katrina's carbon footprint. Science 318:2

Congalton RG, Green K (2009) Assessing the accuracy of remotely sensed data—principles and practices, 2nd edn. CRC Press, Taylor Francis Group, Boca Raton

Dahal D, Liu S, Oeding J (2014) The carbon cycle and hurricanes in the United States between 1900 and 2011. Sci Rep 4:5197

Dale VH, Joyce LA, McNulty S, Neilson RP, Ayres MP, Flannigan MD (2001) Climate change and forest disturbances. Bioscience 51:723

Doswell CA, Burgess DW (1988) On some issues of United States tornado climatology. Mon Weather Rev 116:495–501

Dotzek N, Schultz DM, Markowski PM (2011) A numerical study of the effects of orography on supercells. Atmos Res 100:457–478

ESRI (2011) ArcGIS Desktop Release 10. Environmental Systems Research Institute

Evans AM, Camp AE, Tyrrell ML, Riely CC (2007) Biotic and abiotic influences on wind disturbance in forests of NW Pennsylvania, USA. For Ecol Manag 245:44–53

Forbes GS (1998) Topographic influences on tornadoes in Pennsylvania. Preprints, 19th conference on severe local storms. Minneapolis, MN, American Meteorological Society, 269–272

Foster D, Boose E (1992) Patterns of forest damage resulting from catastrophic wind in central New England, USA. J Ecol 80:79–98

Foster DR, Knight DH, Franklin JF (1998) Landscape patterns and legacies resulting from large, infrequent forest disturbances. Ecosystems 1:497–510

Godfrey CM, Peterson CJ (2014) Estimating enhanced Fujita scale levels based on forest damage severity. Preprints, 24th Conference on severe local storms: the current state of the science and understanding impacts. Atlanta, GA, American Meteorological Society, P832

Gray AN, Spies TA (1996) Gap size, within-gap position and canopy structure effects on conifer seedling establishment. J Ecol 84:635–645

Holland AP, Riordan AJ, Franklin EC (2006) A simple model for simulating tornado damage in forests. J Appl Meteorol Climatol 45:1597–1611

Krueger L, Peterson C (2006) Effects of white-tailed deer on *Tsuga canadensis* regeneration: evidence of microsites as refugia from browsing. Am Midl Nat 156:353–362

Lewellen DC (2012) Effects of topography on tornado dynamics: a simulation study. Preprints, 26th conference on severe local storms. Nashville, TN, USA, American Meterological Society, 4B.1

Li H, Reynolds JF (1994) A simulation experiment to quantify spatial heterogeneity in categorical maps. Ecology 75:2446

Lindemann J, Baker W (2001) Attributes of blowdown patches from a severe wind event in the Southern Rocky Mountains, USA. Landscape Ecol 16:313–325

Lindemann JD, Baker WL (2002) Using GIS to analyse a severe forest blowdown in the Southern Rocky Mountains. Int J Geogr Inf Sci 16:377–399

Lorimer CG (1980) Age structure and disturbance history of a southern Appalachian virgin forest. Ecology 61:1169–1184

Lyza AW, Knupp K (2014) An observational analysis of potential terrain influences on tornado behavior. In: 27th Conference on severe local storms. American Meteorolgoical Society, Madison, WI. 11A.1A

Matlack GR, Gleeson SK, Good RE (1993) Treefall in a mixed oak-pine coastal plain forest: immediate and historical causation. Ecology 74:1559–1566

McGarigal K, Cushman SA, Ene E (2012) FRAGSTATS v4: Spatial pattern program for categorical and continuous maps. Computer software program produced by the authors at the University of Massachusetts, Amherst. Available at http://www.umass.edu/landeco/research/fragstats/fragstats.html

McNab WH, Greenberg CH, Berg EC (2004) Landscape distribution and characteristics of large hurricane-related canopy gaps in a southern Appalachian watershed. For Ecol Manag 196:435–447

Millikin CS, Bowden RD (1996) Soil respiration in pits and mounds following an experimental forest blowdown. Soil Sci Soc Am J 60:1951–1953

Nagendra UJ, Peterson CJ (2015) Plant-soil feedbacks differ in intact and tornado-damaged areas of the southern Appalachian mountains, USA. Plant Soil 4:1–14

Negrón-Juárez R, Baker DB, Chambers JQ, Hurtt GC, Goosem S (2014) Multi-scale sensitivity of Landsat and MODIS to forest disturbance associated with tropical cyclones. Remote Sens Environ 140:679–689

NOAA (2011) Service Assessment: the historic tornadoes of April 2011. Available at http://www.nws.noaa.gov/om/assessments/pdfs/historic_tornadoes.pdf

Nowacki G, Kramer M (1998) The effects of wind disturbance on temperate rain forest structure and dynamics of southeast Alaska

Peterson CJ (2000) Catastrophic wind damage to North American forests and the potential impact of climate change. Sci Total Environ 262:287–311

Peterson CJ, Godfrey CM (2014) Side-by-side tree and house damage in the May 2013 Moore, OK EF-5 tornado: lessons for the enhanced Fujita scale. Preprints, 24th Conference on Severe Local Storms, Atlanta, GA, American Meteorological Society, P831

Peterson CJ, Pickett STA (1995) Forest reorganization: a case study in an old-growth forest catastrophic blowdown. Ecology 76:763–774

Peterson CJ, Krueger LM, Royo AA, Stark S, Carson WP (2013) Disturbance size and severity covary in small and mid-size wind disturbances in Pennsylvania northern hardwoods forests. For Ecol Manag 302:273–279

Pickett STA, White PS (1985) The ecology of natural disturbance and patch dynamics. The ecology of natural disturbance and patch dynamics. Academic Press, Orlando, pp 3–13

Rebertus A, Meier A (2001) Blowdown dynamics in oak-hickory forests of the Missouri Ozarks. J Torrey Bot Soc 128:362–369

Runkle JR (1982) Patterns of disturbance in some old-growth mesic forests of eastern North America. Ecology 63:1533–1546

Schnitzer SA, Carson WP (2001) Treefall gaps and the maintenance of species diversity in a tropical forest. Ecology 82:913–919

Storm Prediction Center (2012) The online tornado FAQ. In: The National Oceanic and Atmospheric Administration. http://www.spc.noaa.gov/faq/tornado/. Accessed 26 Nov 2012

Turner M, Romme W, Gardner R (1993) A revised concept of landscape equilibrium: disturbance and stability on scaled landscapes. Landscape Ecol 8:213–227

Turner MG, Hargrove WW, Gardner RH, Romme WH (1994) Effects of fire on landscape heterogeneity in Yellowstone National Park, Wyoming. J Veg Sci 5:731–742

Turner MG, Romme WH, Tinker DB (2003) Surprises and lessons from the 1988 Yellowstone fires. Front Ecol Environ 1:351–358

Ulanova NG (2000) The effects of windthrow on forests at different spatial scales: a review. For Ecol Manag 135:155–167

U.S. Geological Survey (2015) The National Map: 3D elevation program. http://viewer.nationalmap.gov

Vaillancourt M-A, De Grandpré L, Gauthier S, Kneeshaw D, Drapeau P, Bergeron Y (2009) How can natural disturbance be a guide for forest ecosystem management? In: Gauthier S, Vaillancourt M-A, Leduc A, De Grandpré L, Kneeshaw D, Morin H, Drapeau P, Bergeron Y (eds) Ecosysteme management in the boreal forest. Presses de l'Université du Québec, Montreal, pp 39–55

Verbout SM, Brooks HE, Leslie LM, Schultz DM (2006) Evolution of the U.S. tornado database: 1954–2003. Weather Forecast 21:86–93

Waldron K, Ruel J (2014) Comparisons of spatial patterns between windthrow and logging at two spatial scales. Can J For Res 749:740–749

Webb SL (1989) Contrasting windstorm consequences in two forests, Itasca State Park, Minnesota. Ecology 70:1167–1180

White PS, Jentsch A (2001) The search for generality in studies of disturbance and ecosystem dynamics. Ecosystems 62:399–450

Wilkinson DW, Crosby MK (2010) Rapid assessment of forest damage from tornadoes in Mississippi. Photogramm Eng Remote Sens 76:1298–1301

Xi W, Peet RK, Urban DL (2008) Changes in forest structure, species diversity and spatial pattern following hurricane disturbance in a Piedmont North Carolina forest, USA. J Plant Ecol 1:43–57

Yuan M, Dickens-Micozzi M, Magsig MA (2002) Analysis of tornado damage tracks from the 3 May tornado outbreak using multispectral satellite imagery. Weather Forecast 17:17